Effect of Stress State and Polymer Morphology on Environmental Stress Cracking in Polycarbonate

Arun Raman, Richard J. Farris, Alan J. Lesser

PSE Department, University of Massachusetts, Amherst, Massachusetts 01002

Received Received 26 February 2002; accepted accepted 22 May 2002

ABSTRACT: Environmental stress crazing or cracking (ESC), a long studied phenomenon, is the brittle failure of glassy thermoplastics, which are normally ductile, under the synergistic action of stress and certain surface active agents. This work involves a study of a polycarbonate—oleic acid system under two novel in-depth conditions: multiaxial stress states and changes in the polymer morphology. Initial uniaxial creep tests showed that the formation of cracks rather than crazes is observed. Multiaxial testing is done using blister tests where the polycarbonate film is stressed using a pressurizing medium to form a blister that is in a biaxial state of stress. Changes in the polymer morphology are induced by orientation of the polymer film. On samples exposed to stress and surface active agents, the stress component that is perpendicular to the direction in which the crazes/cracks form appears to influence the crack patterns. The polymer orientation has a significant influence. The orientation not only induces crack formation in a direction parallel to the orientation (regardless of the direction of the major principal stress), but it also reduces the stress required for crack formation for all stress states. Any attempt at modeling the phenomenon of environmental stress cracking therefore needs to take these effects into account. © 2003 Wiley Periodicals, Inc. J Appl Polym Sci 88: 550–564, 2003

Key words: thermoplastics; environmental stress cracking; biaxial stress state; morphology; swelling

INTRODUCTION

Polymers that are normally ductile can fail in a brittle manner under the combined effects of external or residual stress and certain surface active agents. This phenomenon is referred to as environmental stress crazing or cracking (ESC). Common surface active agents that cause ESC include low molecular weight surfactants, solvents, and so forth. Most of these systems involve the physical effects of the interaction between the polymer and the surface active agent and not necessarily the chemical degradation effects.

The ESC problem has been studied for over 50 years. Maxwell and Rahm,[1] for example, noted that the critical strain for crazing of polystyrene is reduced in the presence of several organic liquids. Russell[2] noted that the absorption of swelling agents was accelerated by stress. Ziegler and Brown[3] showed that the kinetics of craze initiation versus the applied strain for polystyrene varied in different media. Craze initiation at any given strain occurred earlier in an organic environment (vapor and liquid), and crazing also occurred at lower strains in that environment.

Correspondence to: A. J. Lesser.

Contract grant sponsors: Motorola; Center for UMass/Industry Research on Polymers; Material Research Science and Engineering Center.

Journal of Applied Polymer Science, Vol. 88, 550–564 (2003)

There have been several hypotheses presented over the years to explain the mechanism of ESC. One such suggestion is that the diffusion of the agent into the polymer and the subsequent stress induced due to the process of swelling is responsible for ESC.[4–8] However, there are enough instances where ESC occurs even in poor solvents where the solvents hardly swell the bulk polymer and where swelling gradients appear nonexistent. Thus, swelling does not account for a general mechanism for ESC. Miller and Visser[9] proposed that solvent crazing of polycarbonate occurred because of stresses arising from crystallization of the polymer induced by swelling. While this might be a correct phenomenological observation for the experiments performed, crystallization due to swelling is still not a generalized mechanism for ESC. Yet another argument is that chain scission is responsible for ESC.[10–12] Chain scission is observed in systems that undergo mechanochemical degradation. ESC is a problem that involves physical interaction effects and not all systems that show ESC undergo chemical degradation.

The two major hypotheses for ESC have been surface energy reduction and plasticization. The surface energy hypothesis[13,14] states that by wetting the surface of holes in a craze, organic agents reduce the energy of craze formation. The plasticization hypothesis states that the solvent and vapor agents reduce the glass transition and thus yield stress near flaw tips, therefore allowing flow processes to occur more

readily. In recent years, Kefalas[15] noted that both of the effects complement each other rather than being mutually exclusive. The strongest evidence for the plasticization mechanism stems from the fact that a correlation has been observed between the critical strain to craze and the extent of the glass-transition temperature (T_g) depression attributable to solvent effects on the polymer. A great deal of work in this direction was performed by Kambour et al.[16–23]

Kambour uniaxially strained a polymer bar using an elliptical cam jig in his experiments.[16–23] The variation in the curvature of the cam along its length produces a strain along the length of each specimen when it is strapped down to the curved surface of the jig. The system is then immersed in a solvent for a prescribed period and temperature. Heavy crazing or cracking was observed in areas under high strain, which became more sparse with distance along the bar and did not occur in areas of low strain. Kambour then defined the critical strain to craze or crack as the strain below which crazes or cracks did not form for the chosen system and set of exposure conditions (time and temperature). Kambour observed from his experiments performed over many different polymer–solvent systems that the critical strain to craze or crack was least in those systems where the polymer and the solvent had similar solubility values (characterized for many systems using Hildebrand's solubility parameter). This was an interesting correlation that led to his widely used expression for a uniaxial craze criterion. Mai[24] reexamined the use of solubility parameters to predict critical strains for ESC and concluded that a good correlation between Hildebrand's solubility parameter and the critical strain was observed in certain systems but not in all. He concluded that, for strongly polar and hydrogen-bonding liquids, 2-dimensional solubility parameter mapping techniques such as used by Jacques and Wyzgoski[25] might have to be used and a priori prediction of the critical strain from solubility parameters was difficult and not possible for all systems.

A number of authors over the years have worked along the lines of Kambour. Wright and Gotham[26] propose a criterion for solvent crazing in which they say that crazing is initiated when the inelastic tensile strain reaches a critical value. The same idea has been developed in recent years by Arnold,[27,28] who supports the idea with some of his experimental data that ESC follows a critical inelastic strain criterion.

A characteristic feature with most of the above work, including that of Kambour, is that in all of them the effect of stress as a tensor is not considered at all. They all deal with the establishment of uniaxial stress or strain criteria. Unfortunately, most applications apply biaxial or multiaxial stresses to the polymer and these stress states are not considered. A quantitative description of the phenomenon of ESC should not only be able to account for generalized polymer–surface active agent systems, but it should also be able to account for generalized states of stress in the material.

A second factor that has not been dealt with extensively in the existing theories on ESC is the effect of morphology and orientation. In many applications, the effect of morphology has proven significant. Yet comparatively little has been done to examine or model this effect.

Kawagoe and coauthors performed studies involving poly(methyl methacrylate) (PMMA) and report that ESC is observed not only under tensile stress but also under compressive and shear stresses.[29,30] This is interesting because ESC has mostly been reported under conditions of tensile stress. They consider diffusion to be the mechanism in their systems. Kawagoe and Kitagawa have also tried to develop a criterion for ESC, modeled over multiaxial stress states, for a PMMA–kerosene system.[31] It is revealed that neither the critical stress bias criterion for crazing as proposed by Sternstein and Ongchin[32] nor the critical strain criterion for crazing as proposed by Oxborough and Bowden[33] explain their ESC results. By considering pressure changes due to the effect of the environmental agent and T_g depression, Kawagoe and Kitagawa[31] develop a criterion that shows a reasonable match with their experimental results. A noticeable feature about the model, though, is that it does not take the thermodynamics of the system undergoing ESC into account at all. Kambour and others have clearly shown that the choice of a particular system, which can be defined in terms of thermodynamic parameters such as the solubility parameter, definitely affects the onset of ESC, depending on the extent to which the polymer and the environmental agent interact with each other. There is no provision in the model developed by Kawagoe and Kitagawa[31] to account for such interaction, given the system parameters a priori. Yet another feature about the model is that, beyond the PMMA–kerosene system, it has not been tested over any other systems. This was a study that did take into account the generalized stress conditions in order to develop a predictive model for ESC, although with shortcomings.

An excellent article by Gent[34] attempts to define the physics governing the phenomenon of ESC. He showed theoretically that a polymer that is exposed to a specific combination of dilatational stress and liquids or vapors can swell in an unstable fashion. The interesting feature about Gent's argument is that he used a dilatational or hydrostatic component of a stress tensor, which takes into account a generalized state of stress rather than just a uniaxial stress. He uses a modified Flory–Huggins equation to relate the volume fraction of solvent in the polymer to the hydrostatic component of stress in the material:

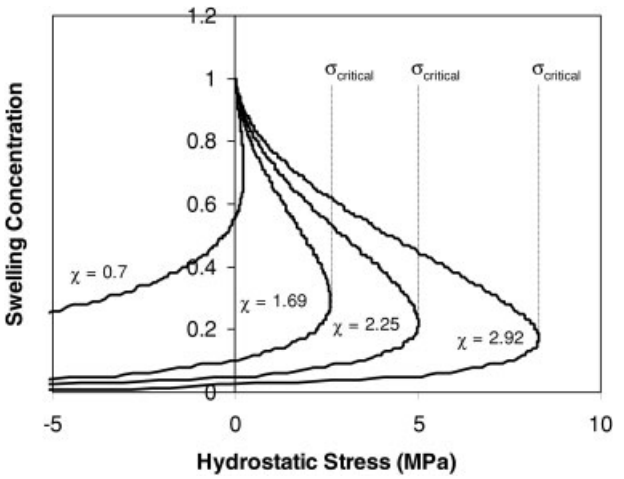

Figure 1 The volume fraction of the solvent in the polymer as a function of the hydrostatic stress for different values of the polymer–solvent interaction parameter.

$$\ln(\phi_s) + (1 - \phi_s) + \chi(1 - \phi_s)^2 + (\rho V_1/M_c) \times [(1 - \phi_s)^{1/3} - (1 - \phi_s)/2] = \sigma_m V_1/RT \quad (1)$$

where ϕ_s is the volume fraction of the solvent in the swollen gel, σ_m is the dilatant (hydrostatic) stress, χ is the polymer–solvent interaction parameter, ρ is the density of the polymer, M_c is the molecular weight of a network chain molecule, V_1 is the molar volume of the solvent, R is the universal gas constant, and T is the temperature. The hydrostatic stress in a material is responsible for volume changes and is a stress tensor with components only on the main diagonal. The magnitude of this component is $(\sigma_{ii}/3)$, where $\sigma_{ii} = \sigma_{11} + \sigma_{22} + \sigma_{33}$, which is the sum of the normal stresses in the overall stress tensor.

It can be seen from a graphical representation of eq. (1) (Fig. 1) that for low values of χ between the polymer and the solvent, that is, for systems where the solvent swells the polymer significantly, even at very low hydrostatic stresses, a compressive stress is required to prevent swelling. If a surface active agent is selected that is not fully compatible (increasing χ values), a critical hydrostatic stress emerges below which little swelling occurs and above which the swelling becomes unbounded. This form of the Flory–Huggins equation has often been successfully used in studies involving swelling of crosslinked rubbers under stress.[35] Gent[34] hypothetically extends this concept to explain the interaction between a glassy polymer and solvent in ESC. According to his theory, because of the relationship between σ_m, ϕ_s, and χ, the material at the tip of the surface concentration points is likely to undergo localized swelling and hence softening, because of the high local dilatant stress. This results in the damage that is observed in ESC. Gent's explanation also accounts for the observation that some of the most potent ESC agents are solvents that do not necessarily swell the polymer in bulk.

One of the objectives of the present work is to study the effect of multiaxial states of stress on ESC in a polycarbonate–oleic acid system, a system with practical ramifications. This is done using a biaxial stress setup. The second objective of this work is to examine how polymer orientation affects ESC and what the effect of the orientation is in conjunction with the effect of multiaxial stress states in the material. From experiments conducted under multiaxial states of stress and experiments conducted using oriented polycarbonate, the possible existence of a constant hydrostatic stress that can be correlated to solvent induced cracks is examined.

EXPERIMENTAL

Materials

Polycarbonate films (0.127 mm thick) were purchased from McMaster Carr. Birefringence measurements showed that these films did not possess any orientation. Oleic acid with a solubility parameter of 7.73 $(cal/mL)^{0.5}$ was purchased from Aldrich.

Orientation

In order to study the effect of orientation in the polymer, polycarbonate sheets (105 × 215 × 0.127 mm) were oriented by drawing using an Instron 5564 equipped with an environmental chamber. The temperature of drawing was maintained at 143°C, which is very close to the T_g of polycarbonate (150°C). The induced orientation was quantified by measuring the birefringence and then calculating the Herman's orientation function (Appendix A).

Biaxial stress setup

Figure 2 shows a schematic of the biaxial testing apparatus. The polycarbonate film is placed between a base and an iron template containing a circular or elliptical hole. A rubber layer that functions as a seal is placed between the polymer film and the iron template. Water is pumped through a small hole in the base using a Cole Parmer 7553-70 peristaltic pump, forcing the film to deform as a blister. The hydrostatic pressure exerted by the water places the portion of the film away from the boundary in a biaxial state of stress. The pressure in the blister is measured with a pressure transducer. The voltage output to the pump head is calibrated and used to measure the flow rate of the water. A National Instruments data acquisition system provides excitation and signal conditioning for the pressure transducer. LabView software is em-

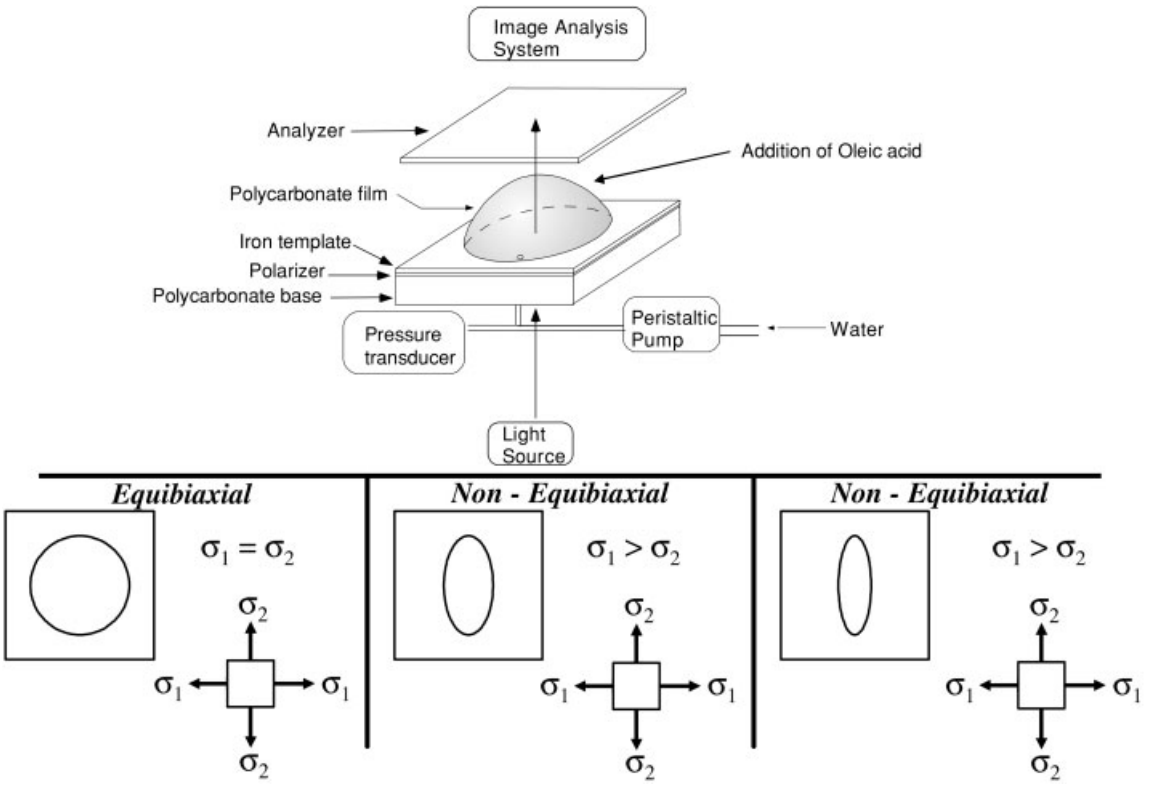

Figure 2 A schematic of the biaxial stress setup. The circular template provides an equibiaxial stress state and the elliptical template provides varying states of nonequibiaxial stress, depending on the ratio of the major to minor axis.

ployed to acquire the pressure and flow-rate signals into a personal computer.

Directions 1 and 2 are defined as the two principal axes. An equibiaxial stress state with principal stresses of the same magnitude ($\sigma_1 = \sigma_2$) is created by using a template with a circular hole (15.2-cm diameter). Nonequibiaxial stress states are created by using templates with elliptical holes. Under nonequibiaxial loading, direction 1 is the direction of the minor axis of the ellipse and direction 2 is the direction of the major axis of the ellipse. From calculations it will also be observed that direction 1 is the direction of the major principal stress and direction 2 is the direction of the minor principal stress. Three nonequibiaxial stress states are studied in this work by using templates with elliptical holes that have major to minor axes of 15.2 $\times$ 10.2, 15.2 $\times$ 7.6, and 15.2 $\times$ 5.1 cm. The above three nonequibiaxial stress states are sometimes referred to herein as 1.5:1, 2:1, and 3:1, respectively, and the equibiaxial stress state is termed 1:1.

The stress and strain values are calculated from the pressure and flow-rate data using the equations in Appendix A. The film is assumed to be a membrane with no in-plane rigidity, and membrane analysis is performed to calculate the expressions for stress and strain from the pressure and volume data. When the circular template is used, an equibiaxial state of stress is created with stress and strain magnitudes in directions 1 and 2 being the same. However, for the nonequibiaxial stress state, the ratio of strain in direction 1 to the strain in direction 2 is approximately the square of the ratio of the major to minor axis of the ellipse. For example, for the 2:1 stress state the ratio ϵ_1 to ϵ_2, where ϵ_i is the strain component in the i direction, is approximately equal to 4/1 and for the 3:1 stress state the corresponding ratio is approximately 9/1. The ratio of principal stresses between directions 1 and 2 depends on the Poisson ratio of polycarbonate, and these equations are presented in detail in Appendix A.

ESC tests

The ESC tests were performed in the following manner. The polycarbonate film was biaxially pressurized using one of the above templates and held at a fixed volume for 10 min during which time the pressure or, equivalently, the stress in the film was allowed to relax. After 10 min, when the pressure attains a constant value, ~0.5 mL of oleic acid was added on the biaxially stressed portion on the blister via a pipette. The surface of the film was then monitored for the onset of crazes or cracks for a fixed amount of time, the choice of which is discussed in the next section. The image of the damage pattern on the polycarbonate surface was captured under cross-polarizers using an optical microscope. If extensive damage was ob-

served, then the experiment was repeated on a fresh sample at a lower pressure. In this manner, the experiments were performed at various stress levels over different stress states. For the uniaxial tests, the strip of polycarbonate (50 × 5 × 0.127 mm) to be tested was stretched in an Instron 5564 with a glass container affixed around the specimen and maintained at a constant strain, during which time the stress in the polymer was allowed to relax in air. After 10 min of stress relaxation, oleic acid was added to the container and the surface monitored for the onset of cracks.

Oriented polycarbonate was also examined in a manner similar to the unoriented polycarbonate: under equibiaxial test conditions, nonequibiaxial (2:1) test conditions, and uniaxial test conditions. In the 2:1 case, the stress was examined for three different loadings of the film orientation perpendicular to the major principal stress, parallel to the major principal stress, and at 45° to both the principal axes.

RESULTS

Orientation measurement

The orientation function for a material is related to the extent of its stretch or draw. In this study, the orientation function for the polycarbonate sheets that were drawn was calculated using birefringence. The unoriented polycarbonate did not show any birefringence. Figure 3(a) shows that the birefringence increases with an increase in the material draw ratio, which is indicative of increased orientation. The maximum birefringence of the polycarbonate drawn at 151°C has been reported to be 0.04.[36] This number is a theoretical maximum and thus can be used to obtain a measure of the Herman's orientation function for the polycarbonate sheets that were oriented in this work [Fig. 3(b)]. With the assumption that polycarbonate is essentially amorphous and does not crystallize significantly on orienting, it is reasonable to assume that the birefringence and the Herman's orientation function provide a measure of the amorphous orientation in the polymer. For the biaxial and uniaxial studies, the oriented polycarbonate sheets that were studied were oriented between 55 and 70% of the theoretical maximum orientation.

Morphological observations

The initial studies involved uniaxial creep tests on unoriented polycarbonate. Strips of unoriented polycarbonate film (50 × 5 × 0.127 mm) were held at a constant stress. These were then exposed to an oleic acid environment and the strain recorded as a function of time (Fig. 4). The surface was monitored for the onset of crazes or cracks, and damage was observed with time. The onset of damage results in the increase

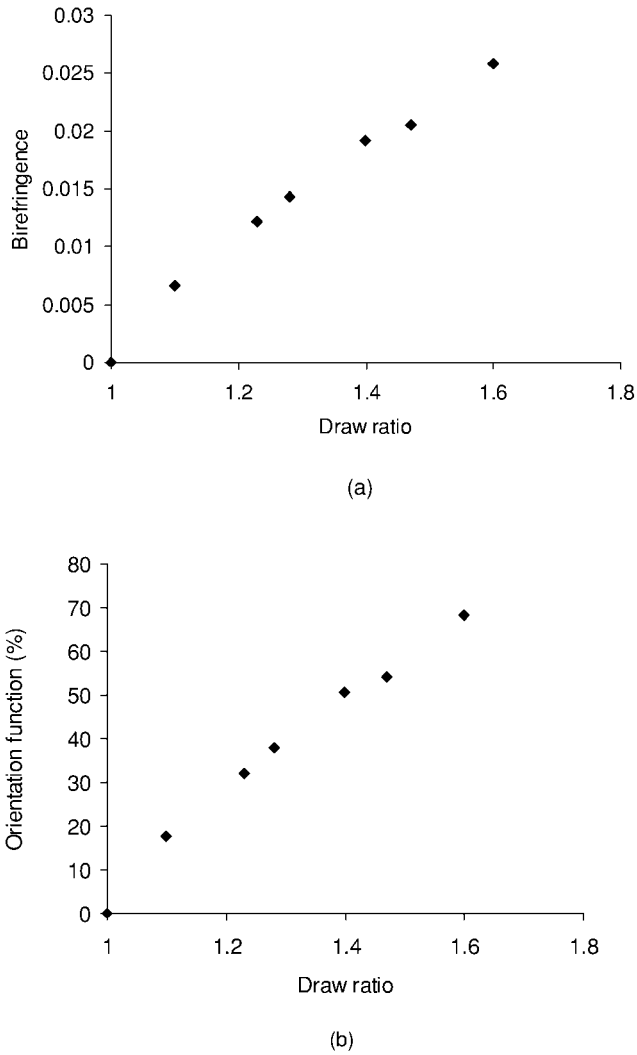

Figure 3 The orientation measurements. (a) The birefringence as a function of the draw ratio for polycarbonate and (b) Herman's orientation function as a function of the draw ratio for polycarbonate.

in strain that is observed with time. Careful examination of the damaged surface under SEM [Fig. 5(a)] reveals that the damage is not actually a craze (i.e., there is no evidence of fibrils). Instead the material between the craze or crack edges is locally drawn, similar to a neck in a uniaxial test. Figure 5(b) is a schematic of the surface when it is viewed from the side. The shallow portions on the surface correspond to material between the craze or crack edges, which results from the localized drawing in these portions.

Crazes are typically precursors to cracks. By definition, crazes contain fibrils. On developing, the craze grows and the fibrils break down, which eventually results in a crack that does not have any fibrils. The fact that the SEM pictures do not show any evidence of fibrils suggests that the damage pattern that results in ESC is not actually a craze but is instead a microcrack. It has been reported in the literature that the

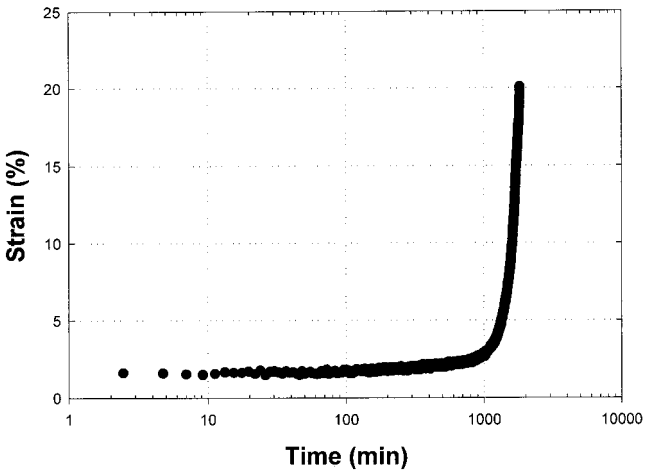

Figure 4 A uniaxial creep test showing the sample strain as a function of time.

crazes formed because of solvent effects are different from air crazes.[37–39] However, what we observe in this work is that the features that are formed because of solvent effects are not actually crazes at all but are instead cracks that contain regions of localized highly drawn material that are not morphologically fibrillar.

Biaxial testing of unoriented polycarbonate

Considering the effects of the stress state, Figure 6 shows typical stress–strain curves for biaxial loading of the polycarbonate films at a constant volumetric loading rate of 20.4 mL/min. Under equibiaxial loading [Fig. 6(a)], the stress and strain values in directions 1 and 2 will be the same. Figure 6(b) is a stress–strain curve for nonequibiaxial loading with the 2:1 elliptical template. The stress and strain values in directions 1 and 2 are shown. Figure 6(c) is a stress–strain curve for nonequibiaxial loading with the 3:1 elliptical template. Note from Figure 6(b,c) that direction 1, which is the minor axis of the ellipse, is the direction of the major principal stress and direction 2, which is the major axis of the ellipse, is the direction of the minor principal stress.

From the ESC experiments that were performed it became apparent very early on that kinetics plays an important role. Even at very low stress values, in the stress range of the experiments performed, cracks always formed on solvent exposure, if provided sufficient time. We found experimentally that at a hydrostatic stress of about 8 MPa under equibiaxial stress conditions, cracks started to form after nearly 20 h of exposure to oleic acid. At higher stress the onset time for crack formation was reduced and the evolution of damage occurred at a higher rate. In addition, for a constant exposure time to the solvent, the cracks that formed at high stresses showed very different patterns from those formed at low stresses. At high stresses a large ensemble of cracks quickly form, unlike at low stress levels where only few cracks form. This transition from a high-ensemble state at a high stress to an isolated state at a low stress happens at a transition stress level. In this work the crack patterns are quantified in terms of this transition stress. We define the transition stress in this study as the stress above which a large ensemble of cracks is formed and below which isolated cracks are formed for 5 min of solvent exposure. The focus of these studies was to observe if, for commensurate exposure conditions over varying states of stress, a constant value for the hydrostatic component of the transition stress may be observed and if that can be correlated to Gent's hypothesis.[34] The above component is referred to herein as the hydrostatic transition stress. The component of the transition stress in the direction perpendicular to the direction in which cracks form, which is referred to herein as the normal transition stress, will also be compared over varying states of stress. It must be mentioned that the experiments were not performed in order to identify if a critical stress exists below which cracks do not form. This was due to the very low values of stress and very long exposure times that would be required for these studies. In fact, the theoretical predictions from Gent's equations for a critical hydrostatic stress for the polycarbonate–oleic acid system is 5.01 MPa.[34] While nothing can be said about the existence or the magnitude of such a critical hy-

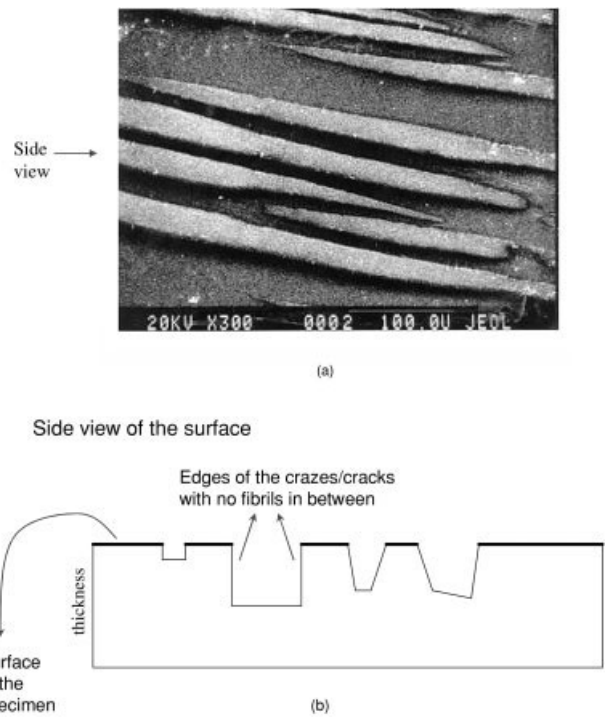

Figure 5 (a) The damaged surface of the SEM image shows cracklike features and no crazes with fibrils. (b) A schematic of the damaged surface when viewed from the side.

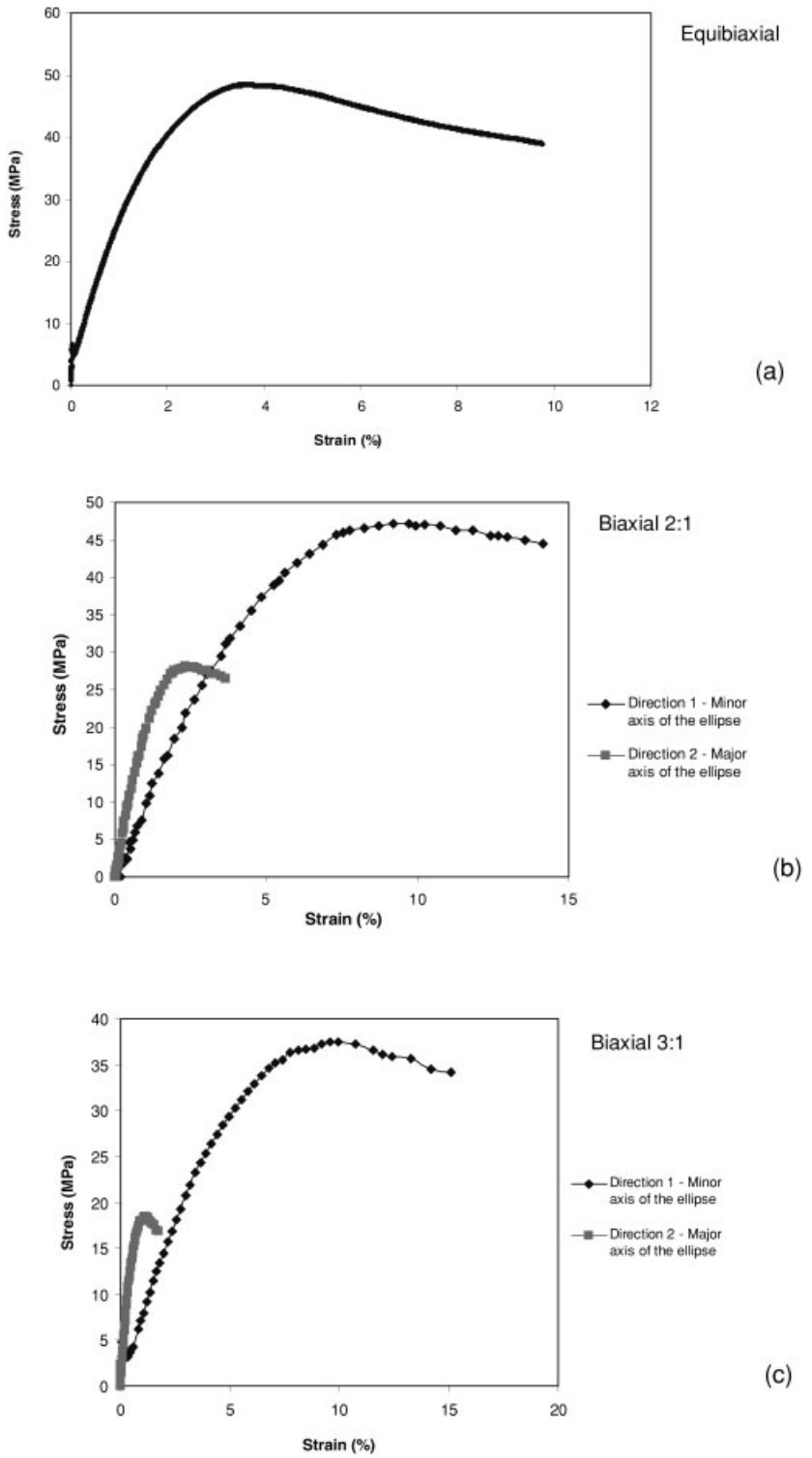

Figure 6 Biaxial stress–strain curves for (a) equibiaxial (1:1), (b) biaxial 2:1, and (c) biaxial 3:1 loadings at the same volumetric flow rate of 20.4 mL/min.

drostatic stress from the experiments performed, the experimental results indicate if a constant hydrostatic or normal stress might exist over various stress states for identical solvent exposure conditions.

Figure 7 shows optical micrographs of three different crack patterns for an equibiaxially stressed specimen. Figure 7(a–c) shows hydrostatic stresses of 25, 20, and 21.5 MPa, which correspond to high, low, and intermediate stresses, the latter being close to the transition stress. The transition from a high-ensemble state to an isolated state can be observed from these images. An important feature to observe under conditions of

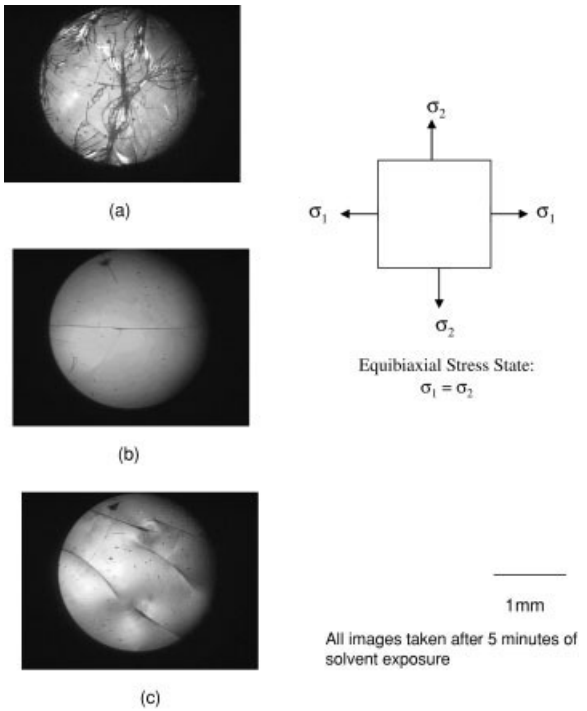

Figure 7 Crack patterns for equibiaxial loading of unoriented polycarbonate after 5 min of solvent exposure for σ_m = (a) 25 (stress greater than transition stress), (b) 20 (stress lower than transition stress), (c) and 21.5 MPa (stress approximately the same as transition stress).

equibiaxial stress on unoriented polycarbonate is that the cracks that are formed are random and in all directions. The cracks show no directional preference. Figure 8(a) shows an image of the damage pattern for a 2:1 biaxially stressed specimen. To recall, for the nonequibiaxial tests, the minor axis of the elliptical template is in the horizontal direction, which is the direction of the major principal stress. As can be seen, the cracks are clearly formed in the vertical direction. A similar pattern is also observed in Figure 8(b,c), which are for specimens that are also nonequibiaxially stressed. These are for 1.5:1 and 3:1 stressed specimens, respectively, with the major principal stress in all cases in the horizontal direction. In contrast to equibiaxial loading, where the cracks are formed in random directions, for nonequibiaxial loading the cracks are always formed in a direction perpendicular to the major principal stress. This is not altogether surprising, because even during uniaxial loading, be it in air or other environments, cracks always form perpendicular to the loading direction. For biaxial loading the cracks are formed perpendicular to the larger load, which is the major principal stress. This is what we observed.

The crack patterns are indicative of a flaw induced mechanism. If there are flaws on the surface of polycarbonate, then these surface flaws will experience greater stress than in the rest of the bulk polycarbonate. As a result, these flaws will act as the sites from where the cracks are initiated. Under greater stress more of these flaws get activated, and so there will be more onset points for crack initiation. This results in the high-ensemble pattern of cracks that is observed. At low stresses fewer of these flaws are activated, and thus there are fewer onset points for the cracks. That results in the isolated state of crack patterns that is observed.

Figure 9 compares the magnitude of the hydrostatic transition stress for the various states of stress. It can be seen that a constant value for the hydrostatic transition stress is not observed over various stress states. It appears that in moving from an equibiaxial state of stress to states that are nonequibiaxial a lower hydrostatic stress is required to cause equivalent crack damage. In fact, the lowest hydrostatic stress is for uniaxial loading. Gent discusses the possible existence of a constant critical hydrostatic stress to explain ESC.[34] As mentioned before, although not much can be said about the existence of a critical hydrostatic stress from the above experimental results, it is however rather clear that it is not possible to define the crack patterns from the experiments studied in terms of a single constant hydrostatic stress over many different states of stress. The hydrostatic transition stress seems to be dependent on the state of stress.

Figure 10 compares the magnitude of the normal transition stress for the various states of stress. It is

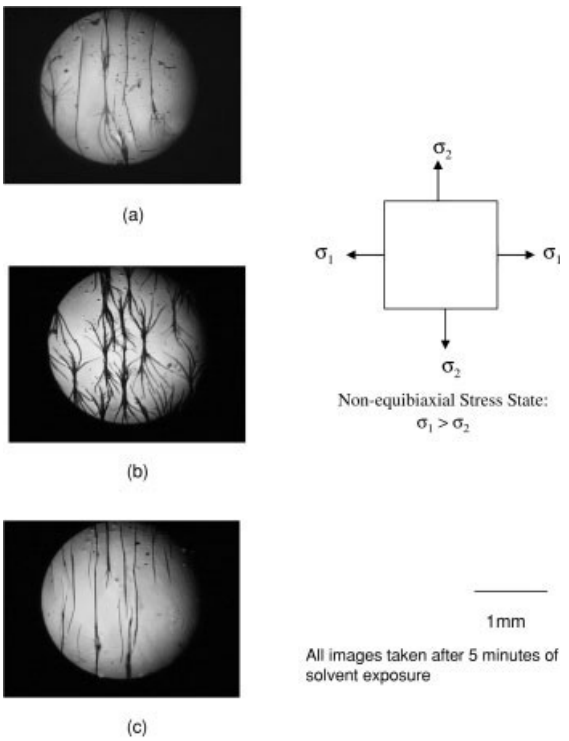

Figure 8 Crack patterns for nonequibiaxial loading of unoriented polycarbonate after 5 min of solvent exposure (stress greater than transition stress for all cases) for (a) 2:1, (b) 1.5:1, and (c) 3:1 samples.

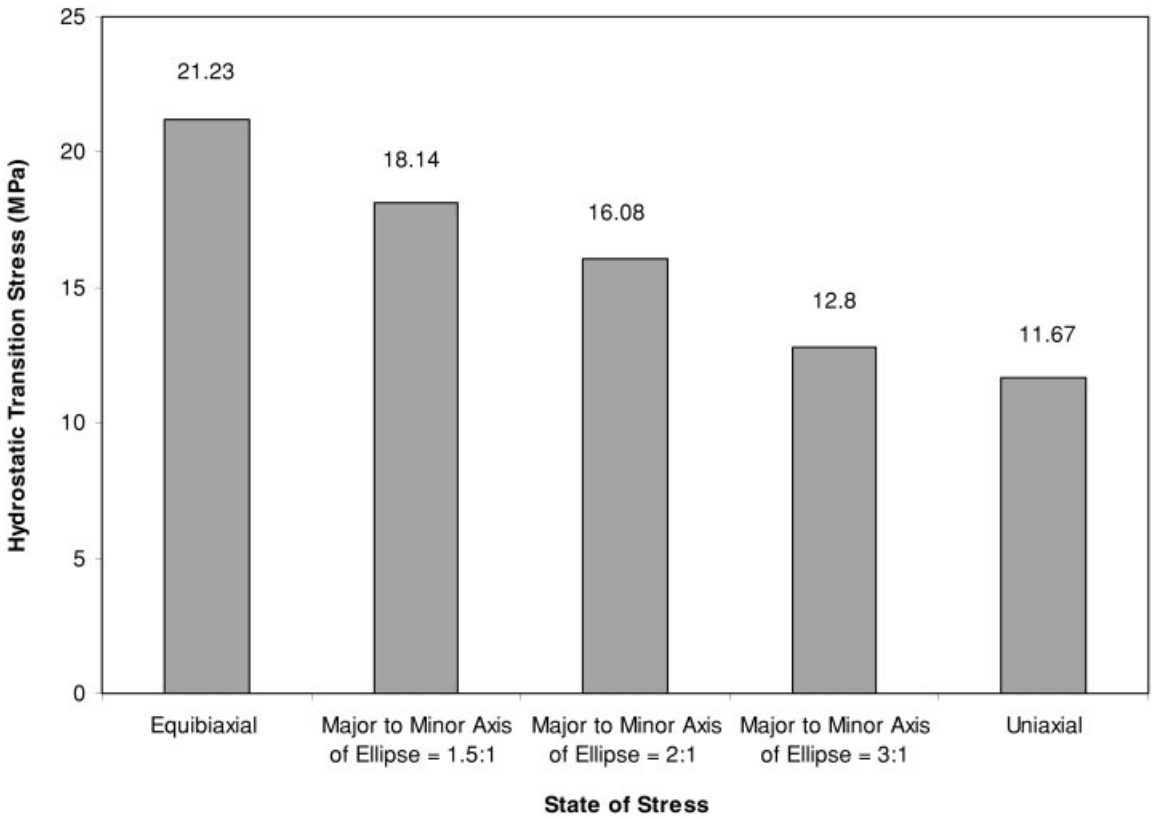

Figure 9 The hydrostatic transition stress to crack for unoriented polycarbonate for different states of stress.

interesting that the normal transition stress does not vary significantly over the various stress states. The approximate normal transition stress over all stress states appears to be 30 MPa. This observation is also supportive of a flaw induced mechanism. In conventional fracture mechanics, where surface flaws influence cracking behavior, the normal stress is the critical parameter that defines crack onset. The normal stress seems to be the determining parameter in the ESC studies performed here over various stress states.

Finally, the trends in the transition stress values were also compared with those presented by Kawagoe and Kitagawa in their work on PMMA–kerosene.[31] That work also involved developing a model on the basis of results obtained from multiaxial conditions of testing. Figure 11 shows a plot of the crazing locus and the model for the Kawagoe–Kitagawa system in terms of the two principal stresses, σ_1 and σ_2. The experimental conditions used in their study were far more elaborate than the conditions used in the current work, because that study also considered experiments that were performed over conditions of shear. In contrast, on a σ_1–σ_2 plot, the experiments performed in our study will correspond only to the first quadrant. The cracking profile for the polycarbonate–oleic acid experiments performed in this study (Fig. 12) shows a curvature similar to Figure 11 for a large portion of the first quadrant. It is important to note that the studies performed by Kawagoe and Kitagawa[31] indicated the existence of a critical stress for crazing for the PMMA–kerosene system. That was not examined in current research for the polycarbonate–oleic acid system. The Kawagoe–Kitagawa model also does not consider the thermodynamics of the system as playing a role, which is not the case, as has been repeatedly shown. Hence, differences between the experimental findings of this research and the Kawagoe–Kitagawa model are not unexpected. It was interesting to see though that the phenomenological observations made from the current study, within the limits in the first quadrant, do show a certain qualitative similarity to what the Kawagoe–Kitagawa model predicted as well.

Biaxial testing of oriented polycarbonate

Figure 13(a) shows optical micrographs of the damage patterns formed under an equibiaxial state of stress for oriented polycarbonate. As mentioned before, these are for samples of polycarbonate that have been oriented to about 55–70% of their theoretical maximum. The cracks are always formed in the direction parallel to the film orientation. This is in contrast to Figure 7(a), where an unoriented film under conditions of equibiaxial stress undergoes cracking randomly and in all directions. Figure 13(b) shows the damage pattern for a 2:1 biaxially stressed specimen with the

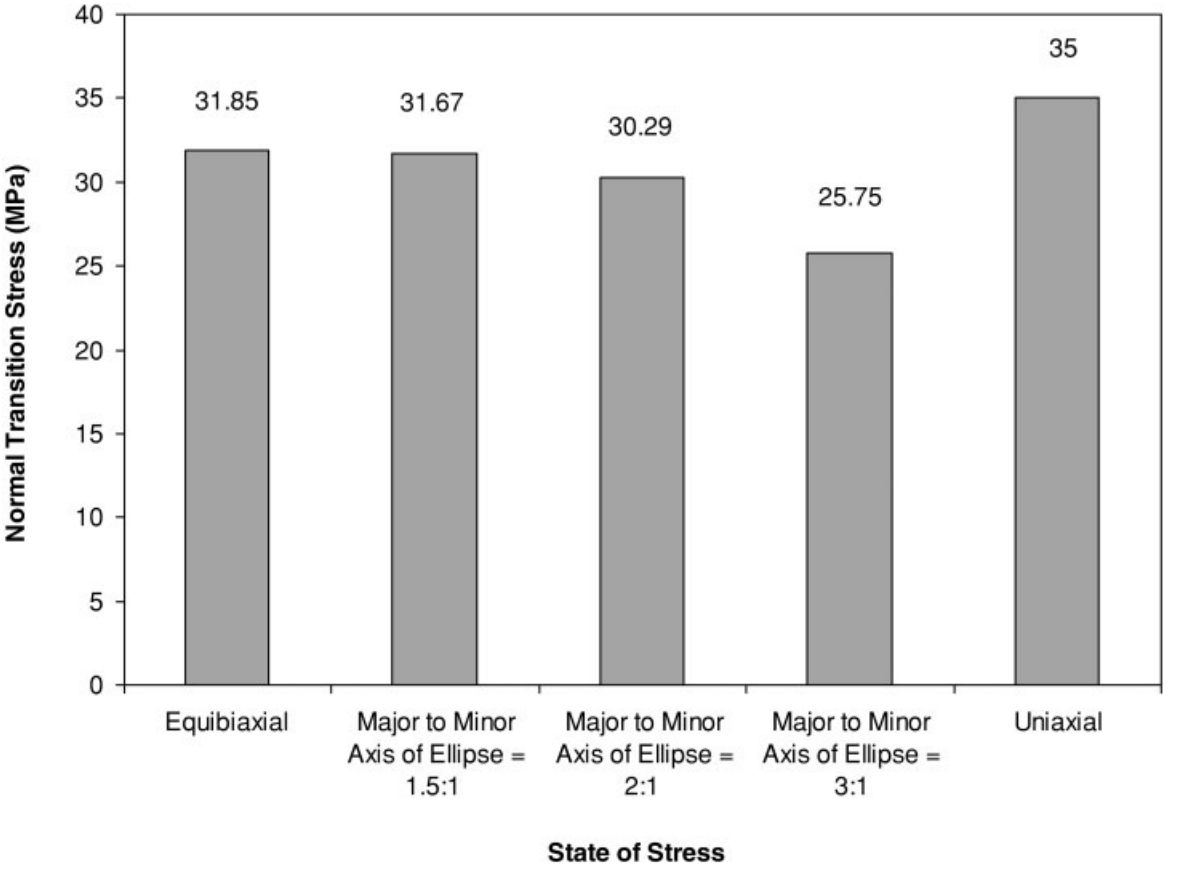

Figure 10 The normal transition stress to crack for unoriented polycarbonate for different states of stress.

orientation in a direction perpendicular to the major principal stress. The cracks are formed in the direction parallel to the film orientation, which is also the direction perpendicular to the major principal stress. Thus, the preferred direction of the cracks is understandable, given the earlier results. The interesting observation comes from Figure 13(c). This is a film that is tested with the film orientation parallel to the major principal stress. In this case, observe that the cracks are formed in the direction that is parallel to the orientation direction but that is not perpendicular to the major principal stress. We observed that, in the case of non-equibiaxial testing of oriented polycarbonate, the cracks always form in the direction parallel to the film orientation and not necessarily in the direction perpendicular to the major principal stress. This was con-

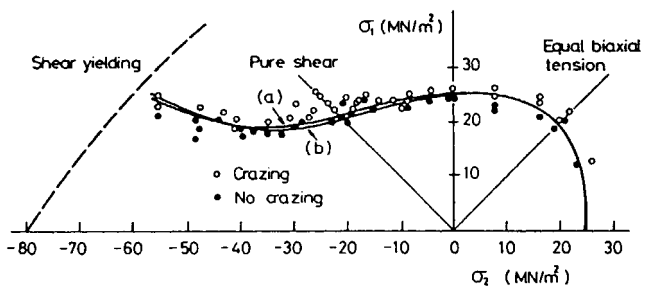

Figure 11 Biaxial crazing data obtained for a PMMA–kerosene system by Kawagoe and Kitagawa[31] on a σ_1–σ_2 plot. The solid curves a and b are calculated from the model developed in that work.

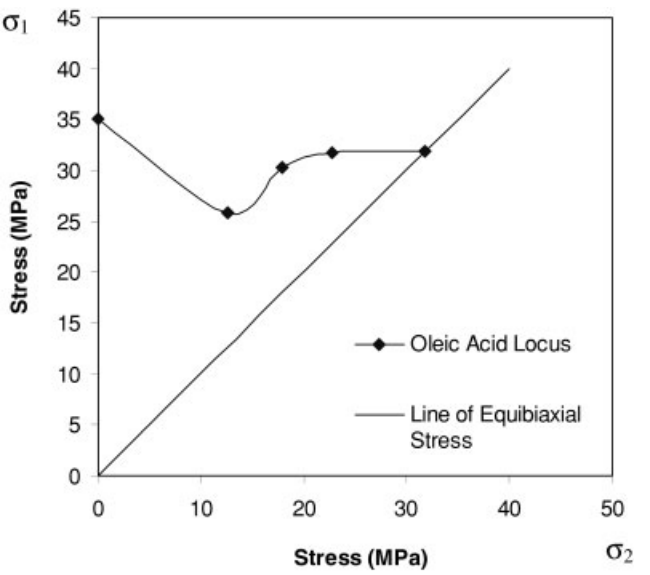

Figure 12 Biaxial cracking data for our polycarbonate–oleic acid system.

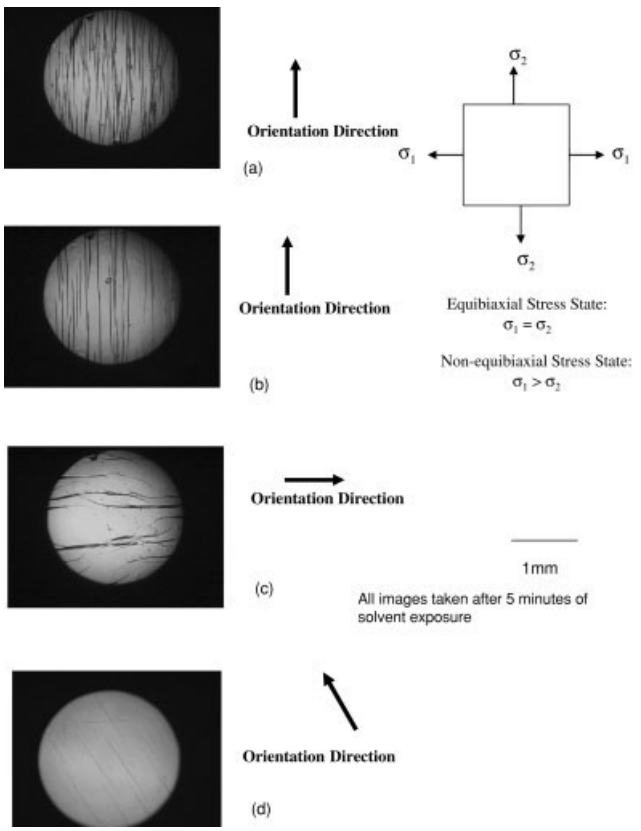

Figure 13 Crack patterns for oriented polycarbonate after 5 min of solvent exposure (stress greater than transition stress for all cases) (a) equibiaxial with orientation in the vertical direction, (b) 2:1 with orientation in the vertical direction, (c) 2:1 with orientation in the horizontal direction, and (d) 2:1 with orientation at 45° to the principal axes.

firmed by examining oriented specimens with the orientation at 45° to both the principal axes. Figure 13(d) shows that the cracks once again are formed in the direction parallel to the orientation.

An examination of the associated transition stress shows that cracking is favored in oriented polycarbonate over unoriented polycarbonate. Figure 14 shows that the hydrostatic component of the transition stress is reduced for oriented polycarbonate under all stress states studied (equibiaxial, biaxial 2:1, and uniaxial) compared to unoriented polycarbonate. Figure 15 shows a similar trend for the normal component of the transition stress. It is very evident from the above observations and results that not only do changes in polymer morphology as induced by orientation play a definite role in inducing crack formation in a particular direction, but the orientation also lowers the required stresses at which these cracks form. It is very interesting from Figure 15 that it appears that for oriented polycarbonate, over all stress states, the normal transition stress values are similar in magnitude. The same cannot be said of the hydrostatic transition stress from Figure 14.

DISCUSSION

The above results from the experiments on multiaxial stress states and oriented polymers bear out two very important consequences in characterizing the phenomenon of ESC. The first is that even over various stress states the stress component normal to the direction in which the cracks form seems to be the important parameter determining ESC. The second consequence is that orientation effects play a role as well. Fabrication and processing of thermoplastics toward their end-use applications results in many of them possessing significant amounts of residual orientation. Our results show that changes in polymer morphology, which are attributable to an increase in orientation, not only influences the direction of cracks but also reduces the stress at which these cracks form. Any model that can be used to predict environmental stress failure therefore must account for the effect of polymer morphology in the governing equations that describe it. The damage patterns that are formed seem to be indicative of a flaw induced mechanism. The flaws are stress concentration points on the surface that act as sites of crack initiation. At low stresses few flaws are activated, resulting in isolated crack patterns. At high stresses there are more onset points, resulting in the high density ensemble that is observed. Our ongoing work involves modeling the phenomenon along the above lines and on the basis of phenomenological observations presented in this work.

CONCLUSIONS

The environmental stress effects that are observed in a polycarbonate–oleic acid system are indicative of the formation of cracks not crazes. The kinetics of the system plays an important role in the onset of cracks: at a high stress the cracks initiate faster than at a low stress. The effect of the stress state is studied. Under high stresses there is a high-ensemble state of cracks, and at low stresses the patterns are more indicative of an isolated crack morphology. This transition between a high stress pattern and a low stress pattern is characterized by a transition stress. From studies over various stress states it appears that the normal transition stress (i.e., the component of the transition stress perpendicular to the direction of cracks) determines the crack patterns that result. It is also observed that for all states of stress, the oriented specimens crack at lower stresses than their unoriented counterpart. The direction of propagation of the cracks is also influenced. In an unoriented polymer the cracks are formed in random directions for an equibiaxially stressed specimen, but they are always perpendicular to the major principal stress for a nonequibiaxially stressed specimen. In an oriented polymer, however, the cracks are always formed parallel to the film ori-

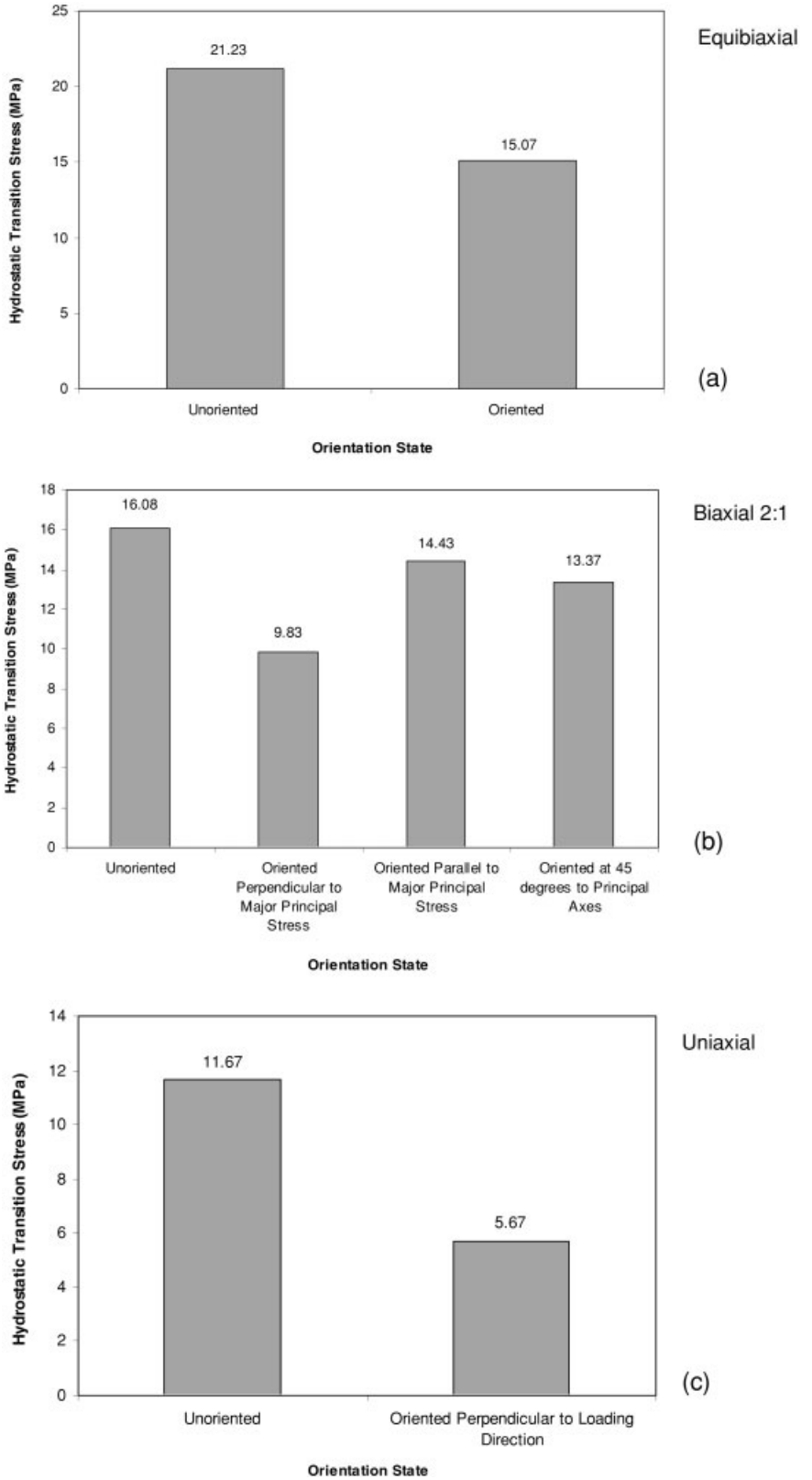

Figure 14 A comparison of the hydrostatic transition stress to crack between oriented and unoriented polycarbonate for (a) equibiaxial, (b) 2:1, and (c) uniaxial stress states.

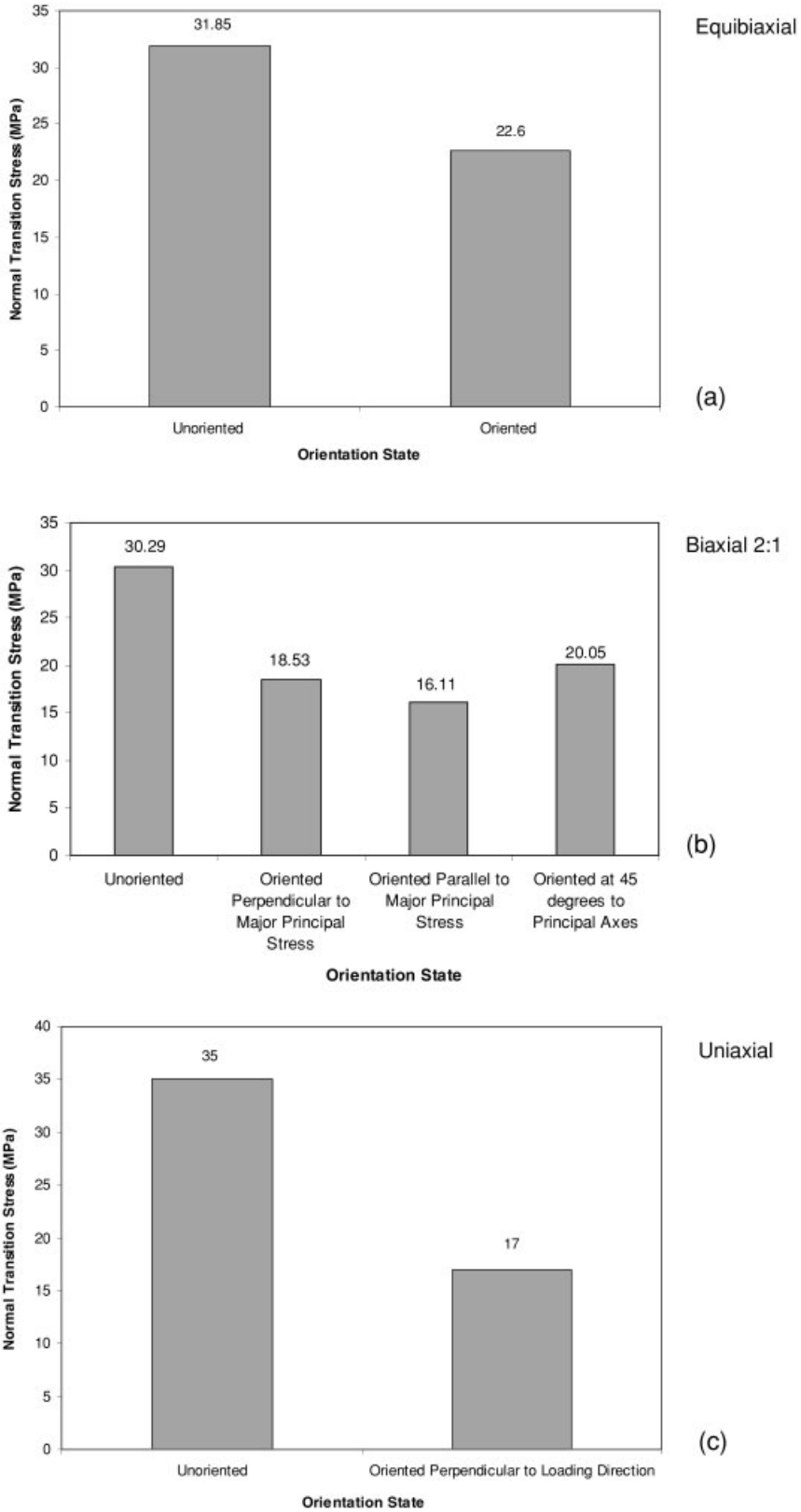

Figure 15 A comparison of normal transition stress to crack between oriented and unoriented polycarbonate for (a) equibiaxial, (b) 2:1, and (c) uniaxial stress states.

entation. Modeling of the phenomenon to develop a generalized predictive failure model is in progress on the basis of the above observations and along the lines of what appears to be a flaw induced mechanism.

The authors wish to acknowledge the financial assistance from Motorola during the early part of this work. Assistance from the Center for UMass/Industry Research on Polymers (CUMIRP) and the Material Research Science and Engineering Center (MRSEC) is also greatly appreciated.

APPENDIX A

Herman's orientation function

Notation

- f Herman's orientation function
- n experimentally measured birefringence
- n_0 maximum birefringence (reported in the literature)

Function for polycarbonate sheets in this study

$$f = \Delta n / \Delta n_0$$

Biaxial loading

Notation

- a radius of circular template for equibiaxial case (semiminor axis of elliptical template for nonequibiaxial case)
- b semimajor axis of elliptical template for nonequibiaxial case
- h height at the center of the blister
- p pressure in the blister
- R_1 radius of curvature of the blister (radius of curvature of the cross section of an ellipsoid along the plane that contains the minor axis for the nonequibiaxial case)
- R_2 radius of curvature of the cross section of an ellipsoid along the plane that contains the major axis for the nonequibiaxial case (same as R_1 for the equibiaxial case)
- V blister volume
- σ_1 stress in direction 1 (major principal stress for nonequibiaxial case)
- ϵ_1 strain in direction 1 (major principal strain for nonequibiaxial case)
- σ_2 stress in direction 2 (minor principal stress for nonequibiaxial case)
- ϵ_2 strain in direction 2 (minor principal strain for nonequibiaxial case)
- ν Poisson's ratio of polycarbonate (assumed to be 0.4 for calculation)

Equibiaxial loading

$$h^3 + 3a^2h = \frac{6V}{\pi}$$

$$R_1 = R_2 = \frac{a^2 + h^2}{2h}$$

$$\sigma_1 = \frac{pR_1}{2t} \quad \text{(same as } \sigma_2 \text{ for equibiaxial case)}$$

$$\varepsilon_1 = \frac{a^2 + h^2}{2ah} \sin^{-1}\left(\frac{2ah}{a^2 + h^2}\right) - 1$$

(same as ε_2 for equibiaxial case)

Nonequibiaxial loading

$$\frac{\pi}{h}\int_0^h \sqrt{a^2 + hz}\ \sqrt{b^2 + hz}(h - z)dz = V$$

$$R_1 = \frac{a^2 + h^2}{2h}$$

$$R_2 = \frac{b^2 + h^2}{2h}$$

$$\varepsilon_1 = \frac{a^2 + h^2}{2ah} \sin^{-1}\left(\frac{2ah}{a^2 + h^2}\right) - 1$$

$$\varepsilon_2 = \frac{b^2 + h^2}{2bh} \sin^{-1}\left(\frac{2bh}{b^2 + h^2}\right) - 1$$

$$\sigma_1 = \frac{(\varepsilon_1 + \nu\varepsilon_2)}{(\varepsilon_1R_2 + \varepsilon_2R_1) + \nu(\varepsilon_1R_1 + \varepsilon_2R_2)} \frac{pR_1R_2}{t}$$

$$\sigma_2 = \frac{(\varepsilon_2 + \nu\varepsilon_1)}{(\varepsilon_1R_2 + \varepsilon_2R_1) + \nu(\varepsilon_1R_1 + \varepsilon_2R_2)} \frac{pR_1R_2}{t}$$

References

1. Maxwell, B.; Rahm, L. F. Ind Eng Chem 1949, 41, 1988.
2. Russell, E. W. Nature 1950, 165, 91.
3. Ziegler, E. E.; Brown, W. E. Plast Technol 1955, 1, 409.
4. Holley, R. H.; Hopfenberg, H. P.; Stannett, V. Polym Eng Sci 1970, 10, 376.
5. Turner, A., Jr.; Gurnee, F. E.; Lloyd, W. G. J Polym Sci Part B Polym Lett 1966, 12, 249.
6. Thomas, N. L.; Windle, A. H. Polymer 1981, 22, 627.
7. Fu, T. Z.; Durning, C. J.; Tong, H. M. J Appl Polym Sci 1991, 43, 709.
8. Berry, B. S.; Pritchet, W. C. IBM J Res Dev 1984, 28, 662.
9. Miller, G. W.; Visser, S. A. D.; Morecroft, A. S. Polym Eng Sci 1971, 11, 73.
10. Jellinek, H. H. G. In Fracture Processes in Polymeric Solids; Interscience Publishers: New York, 1964; Chapter IV.
11. Charlesby, A. In Fracture Processes in Polymeric Solids; Interscience Publishers: New York, 1964; Chapter IV.

12. Kambour, R. P. Proceeding of the International Conference on Corrosion, 1971.
13. Stuart, H. A.; Markowski, G.; Jeschke, D. Kunststoffe 1964, 54, 618.
14. Bergen, R. L., Jr. SPE J 1968, 24, 77.
15. Kefalas, V. A. J Appl Polym Sci 1995, 58, 711.
16. Kambour, R. P. Macromol Rev 1973, 7, 1.
17. Kambour, R. P. Encyclopedia of Polymer Science and Engineering; 1986; Vol. 4, p. 299.
18. Kambour, R. P.; Gruner, C. L.; Romagosa, E. E. Macromolecules 1974, 7, 248.
19. Kambour, R. P.; Gruner, C. L. J Polym Sci Polym Phys Ed 1978, 16, 703.
20. White, S. A.; Weissman, S. R.; Kambour, R. P. J Appl Polym Sci 1982, 27, 675.
21. Kambour, R. P.; Gruner, C. L.; Romagosa, E. E. J Polym Sci Polym Phys Ed 1973, 11, 1879.
22. Kambour, R. P.; Romagosa, E. E.; Gruner, C. L. Macromolecules 1972, 5, 335.
23. Kambour, R. P.; Bernier, G. A. J Chem Phys 1968, 1, 393.
24. Mai, Y. W. J Mater Sci 1986, 21, 904.
25. Jacques, C. H. M.; Wyzgoski, M. G. J Appl Polym Sci 1979, 23, 1153.
26. Wright, D. C.; Gotham, K. V. Polym Eng Sci 1983, 23(3), 135.
27. Arnold, J. C. Plast Rubber Compos Process Appl 1998, 27(3), 139.
28. Arnold, J. C. J Mater Sci 1995, 30, 655.
29. Kawagoe, M.; Kitagawa, M. J Mater Sci 1987, 22, 3000.
30. Kawagoe, M.; Morita, M. J Mater Sci 1993, 28, 2347.
31. Kawagoe, M.; Kitagawa, M. J Polym Sci Polym Phys Ed 1981, 19, 1423.
32. Sternstein, S. S.; Ongchin, L. Polym Prepr Am Chem Soc Div Polym Chem 1969, 10, 1117.
33. Oxborough, R. J.; Bowden, P. B. Philos Mag 1973, 28, 547.
34. Gent, A. N. J Mater Sci 1970, 5, 925.
35. Treloar, L. R. G. The Physics of Rubber Elasticity; Clarendon Press: Oxford, UK, 1975.
36. Inoue, T.; Okamoto, H.; Osaki, K. Macromolecules 1992, 25, 7069.
37. Kramer, E. J. In Developments in Polymer Fracture; Andrews, E. H., Ed.; Applied Science: London, 1979; Vol. 1, Chapter 3.
38. Thomas, E. L.; Israel, S. J. J Mater Sci 1975, 10, 1603.
39. Lagaron, J. M.; Pastor, J. M.; Kip, B. J. Polymer 1999, 40, 1629.